Prediction of the continuous cooling transformation diagram of some selected steels using artificial neural networks

Willem Vermeulen, Sybrand van der Zwaag, Peter Morris and Ton de Weijer

Continuous cooling transformation (CCT) diagrams play an important role in the description of the transformation behaviour of steels. The experimental determination of a CCT diagram is a very time consuming and expensive task. It would therefore be very attractive to be able to predict CCT diagrams from the chemical composition of the steel and its austenitising temperature. In this article the use of artificial neural networks for the prediction of the transformation start and finish lines in CCT diagrams is described. The data were selected from a single source: The vanadium steels, atlas of continuous cooling transformation diagrams [4].
Three neural networks with different numbers of hidden nodes (5-10-15) were trained. The number of hidden nodes did not significantly influence the accuracy in the prediction. The network with the least number of hidden nodes (5) was therefore chosen for the evaluation of the performance of the neural networks. This neural network was able to predict the general trends in the CCT diagrams quite well. The relative standard deviation in the prediction of start and end temperatures of each transformation depended on the cooling rate. For the high and low cooling rates it was ~ 40 °C, for the intermediate it rose to 90 °C for the ferrite start formation and to 75 °C for the other diffusional transformations (pearlite and bainite).
The accuracy of the predicted CCT diagram was primarily restricted by the modest quality of the input data used to train the neural network.

Vorausberechnung kontinuierlicher ZTU-Diagramme einiger ausgewählter Stahlsorten mit künstlichen neuronalen Netzen. Kontinuierliche ZTU-Schaubilder spielen bei der Beschreibung des Umwandlungsverhaltens von Stahl eine bedeutende Rolle. Die experimentelle Bestimmung eines solchen Diagramms ist zeitintensiv und teuer. Daher wäre eine Ableitung dieser Diagramme aus der chemischen Zusammensetzung des Stahls und seiner Austenitisierungstemperatur hochinteressant.
In der vorliegenden Arbeit wird die Anwendung neuronaler Netze zur Vorausberechnung der Umwandlungsstart- und -endtemperaturen in kontinuierlichen ZTU-Schaubildern beschrieben. Die Daten stammen aus einer einzigen Quelle, dem Atlas kontinuierlicher ZTU-Schaubilder für Vanadinstähle [4].
Drei neuronale Netze mit unterschiedlich vielen verdeckten Knoten (5-10-15) werden trainiert. Die Anzahl der mittleren Knoten beeinflußt die Vorhersagegenauigkeit nicht merklich, daher wurde ein Netz mit 5 gewählt. Es eignete sich recht gut zur Ermittlung der allgemeinen Trends in kontinuierlichen ZTU-Diagrammen. Die Standardabweichung für Start- und Endtemperaturen jeder Umwandlung hing von der Abkühlgeschwindigkeit ab: für hohe und niedrige Abkühlgeschwindigkeiten betrug sie ~ 40 °C, im mittleren Bereich stieg sie auf 90 °C (Beginn der Ferritbildung) bzw. 75 °C für andere diffusionsgesteuerte Umwandlungen (Perlite oder Bainit).
Die Genauigkeit der so aufgestellten ZTU-Schaubilder wird von der Qualität der für das Training des neuronalen Netzes benutzten Eingangsdaten beschränkt.

Heat treatment of steel plays an important role in the engineering industry in general. Success in heat treatment requires that the operating variables, in particular those concerned with the quenching process and the hardenability of the steel, can be carefully controlled. Thus, knowledge of hardenability and phase transformations in steels are essential to produce a steel with the desired properties [1].

The hardenability of steels is well characterised by the Jominy end-quench-test, while the transformation kinetics of steels usually are described using either isothermal transformation (IT or TTT) or continuous cooling transformation (CCT) diagrams. TTT diagrams describe the phase transformations at a constant temperature, while CCT diagrams describe the transformations taking place during continuous cooling at various constant cooling rates. The latter diagrams resemble more closely the conditions during the actual production process of the steel or during its heat treatment at a later stage. The CCT diagrams not only provide information on the transformation start and finish conditions, but also on the resulting hardness and microstructures for each particular cooling curve.

The effort to determine a CCT diagram experimentally is considerable. Normally, a CCT diagram is determined using dilatometry in combination with microstructural studies. This is a very time consuming and often difficult task and it would therefore be very attractive if it were possible to predict the CCT diagram of a particular steel from its chemical composition and its prior thermal history. Of particular interest would be the prediction of the transformation start and finish temperature and it is to this information in the CCT diagram to which this work is restricted.

At present, the problem is approached in two ways; theoretically using physical models, or statistically, using earlier CCT diagrams determined for similar steel grades. The theoretical approach might prove to be valuable for an accurate CCT diagram prediction in the long run. However, some aspects of the transformation are not yet fully understood (at least not in a quantitative manner) and this poses an obstacle to the theoretical approach. The statistical approach has not been very successful either, because of the complexity of the problem.

Ir. Willem Vermeulen; Professor Dr. Ir. Sybrand van der Zwaag, Delft University of Technology, Materials Science Laboratory, Delft; *Dr. Ton de Weijer,* AKZO Nobel Research, Corporate Research Laboratory, Arnhem, Netherlands; *Dr. Peter Morris,* British Steel plc, Swinden Technology Centre, Rotherham, England.

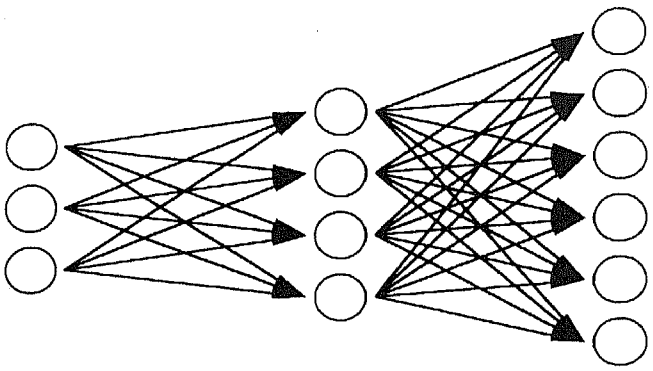

Figure 1. Hierarchical feed-forward neural network. Data are transfered from left to right along the arrows; the circles represent the nodes or neurons

The purpose of this report is to describe the use of artificial neural networks for predicting the transformation start and finish lines in a CCT diagram from the steel composition and the austenitising temperature. Neural networks are most suitable for analysing complex data sets with unknown and/or non-linear dependencies between input and output parameters. They have previously been used with success to predict the martensite start temperature [2] and the Jominy hardness profile [3]. Following a general description of the neural network theory, the data selection and processing for this particular problem is described in more detail. The data to develop the model were selected from a collection of several continuous cooling diagrams for different vanadium steels from open literature [4]. The optimal architecture for the CCT diagrams was determined and the results of this neural network are presented. The quality of predicted CCT diagrams is illustrated for three different steel grades. Furthermore, the influence of the carbon and manganese content on the Ar_3 temperature is discussed in more detail.

The neural network

In this section, the very basics of the type of neural network used will be discussed. No attempts are made to present a full overview of all types of neural networks, nor to discuss the theory of the type of neural network used in the finest detail. For those interested in a general overview or in the finest detail, some excellent books are available [5...8].

In this research, a hierarchical feed-forward neural network is used. A diagram of this type of neural network is shown in **figure 1.** The basic unit in a neural network is its processing element, called a node or a neuron. In a hierarchical neural network these nodes are ordered in layers. The network is called feed-forward, because the nodes process the information in one direction only, from input to output. Each node in a layer is connected, via a weight factor, with each node in the preceding layer; the network is fully connected. The number of nodes in the input layer equals the number of input parameters. The number of nodes in the output layer equals the number of output parameters. The optimum number of nodes in the intermediate -hidden- layer depends on the complexity of the problem, and it is up to the researcher to determine this. This intermediate layer is called the hidden layer, since both inputs and outputs from this layer come and go from other network layers and hence this layer is not seen when looking from the outside to the network. The number of input, output, and hidden nodes and their connections define the architecture of the neural network.

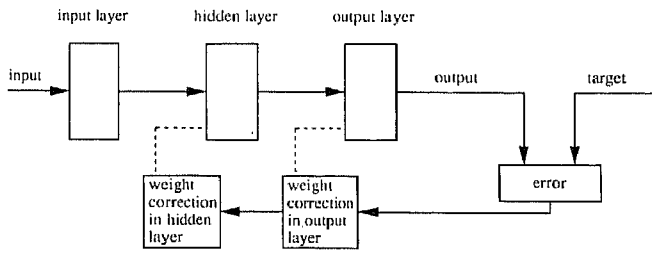

Figure 2. Flowchart of a training cycle in a hierarchical feed-forward neural network

Each node computes the scalar product of its input values and their weight factors and passes this value to a sigmoid transfer function, which produces the output signal of the node. To determine the weight factors -the actual modelling- the neural network has to be trained. Hierarchical feed-forward neural networks are trained under so-called supervision. A wide variety of different training rules for supervisional training have been reported in literature and it is beyond the scope of this work to discuss them here in detail. A detailed description of network training rules or neural networks in general can be found in references [5...8]. Only the general concept of supervised training will be discussed here.

An iteration in the training cycle is outlined in the flowchart of **figure 2.** To start, the weight factors are initialised randomly. Then, the input and output data of one sample are presented to the network, which, with its randomly initialised weight factors, calculates the output of the sample; the predicted value. This predicted value is compared with the actual or target value of the sample. The difference between target and predicted value -the error in the prediction- is a measure for the weight factor correction. This correction takes place in the reverse direction - back propagation of error- so first, the weight factors of the output layer are corrected, and then the weight factors of the nodes in the hidden layer. Once the weight factors have been corrected for all samples, the training cycle is repeated until the differences between calculated and target output values are minimised sufficiently.

When there is a large number of training cycles - iterations- the network starts to model not only the functional dependencies between input and output parameters but also the noise in the data set. This is called overtraining. To prevent the network from overtraining the data is split into a relatively large training set and a smaller test or validation set. The weight factors in the network are adjusted using the data in the training set only. In case of overtraining the error for the training set decreases while that for the test set increases with further iteration. At this point training should be stopped. Our neural network software program is designed in such a way that at the onset of overtraining the training is stopped automatically. Once the network is trained, the weight factors are fixed and the

neural network can be used to calculate the output for any arbitrary set of input data.

Data selection and processing

As the correct experimental determination of CCT diagrams is by no means trivial, a large scatter exists in CCT diagrams for nominally the same steel grade. To minimise this scatter all data used in the present work are selected from a single source; The vanadium steels, atlas of continuous cooling transformation diagrams [4]. In total 89 steel grades were selected for training and validation of the neural network. Only those CCT diagrams with connected phase transformation fields were selected. A typical CCT diagram of a steel used for training and its chemical composition is shown in **figure 3.**

The input parameters of all neural networks were the chemical composition and the austenitising temperature. The chemical composition was characterised using 12 alloying elements: C, Mn, Si, S, P, Cr, Ni, Mo, V, Cu, Al, and N. The prior austenite grain size has an important effect on the transformation kinetics [9], but as no information was available on this parameter, it could not be included as an input parameter. Instead, the austenitising temperature was used as a qualitative measure for grain size effects. The input parameter ranges (austenitising temperature and alloying element concentrations) for the neural networks are given in **table 1.**

The output of the neural network was the transformation lines in the CCT diagram.

The CCT diagrams had to be converted from graphical to numerical format, because only numerical formats can be handled by the type of neural network used.

Several options were open to characterise the CCT diagrams numerically:

1. divide the CCT diagram into squares with equal surface area and determine the microstructure that is stable within each square;
2. determine the intercepts of fixed isotherms with the boundary lines indicating the time-temperature combination leading to a particular transformation product;
3. determine the intercepts of fixed isochrons with the boundary lines indicating the time-temperature combination leading to a particular transformation product;
4. determine the intercepts of fixed continuous cooling curves with the boundary lines indicating the time-temperature combination leading to a particular transformation product.

The advantages and disadvantages for the various options are discussed below.

The option to divide the CCT diagram into small uniform squares (option 1) is not feasible since the amount of redundant data to be processed becomes very large if a high resolution is required.

For all intercept methods (options 2 to 4) a similar approach can be used. This approach is to determine the intercepts of a test-line (isothermal, isochronal or cooling curve) with the boundary lines in the CCT diagram indicating the time-temperature combination leading to a particular phase transformation.

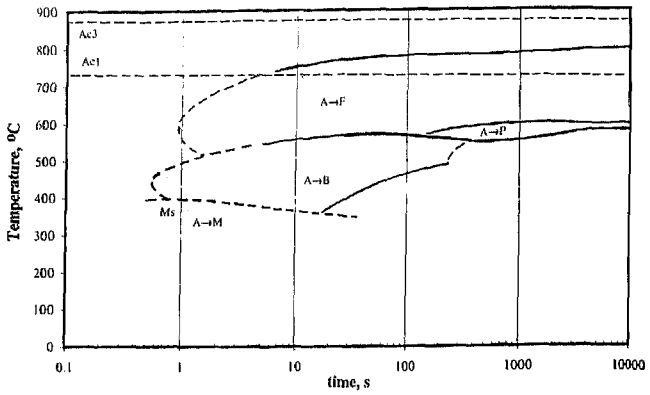

Figure 3. CCT diagram for a 0.14% C, 1.52% Mn, 0.48% Si, 0.004% S, 0.011% P, 0.071% V steel [4]

The intercept method using the fixed number of isotherms (option 2) resembles the conditions during the determination of a TTT diagram best. Option 4, using the fixed number of cooling curves resembles the conditions during the determination of a CCT diagram best and this method was therefore chosen to characterise the CCT diagram. In our model 23 Newtonian curves were superimposed on each CCT diagram and the intercepts were determined. The cooling rates corresponding to these curves ranged from 720 to 0.05 C/s. In **figure 4** a CCT diagram of a hypothetical steel is shown, as well as five out of the total 23 different cooling rates, indicated with dotted lines.

A particular complication in this procedure, which would be present in any other of the intercept methods, is that the number of intercepts is not a constant but may vary with the cooling rate and the steel composition. Furthermore, the order of the intercept points along a particular cooling curve is not uniquely related to a particular type of transformation. For example, the first intercept at the highest cooling rate is usually related to the martensite formation, while the first intercept at the lowest cooling rate is related to the ferrite formation.

As for any statistical modelling, including the neural network modelling, the number of dependent variables should be constant and uniquely defined, the number of intercepts for each cooling curve was fixed artificially at 6:

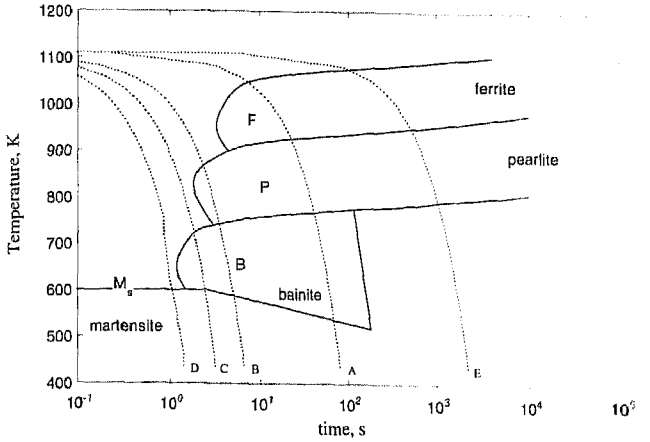

Figure 4. CCT diagram of a hypothetical steel. The labels in the figure refer to conditions discussed later on

1 time-temperature combination for the start of the ferrite formation (ferrite start temperature),
2 time-temperature combination for the end of the ferrite formation (ferrite end temperature),
3 time-temperature combination for the start of the pearlite formation (pearlite start temperature),
4 time-temperature combination for the end of the pearlite formation (pearlite end temperature),
5 time-temperature combination for the start of the bainite formation (bainite start temperature),
6 time-temperature combination for the end of the bainite formation (bainite end temperature).

Now, several transformation scenarios are possible when converting CCT diagrams to a numerical format:

- if for a particular cooling rate the austenite transforms to ferrite, pearlite and bainite, the time-temperature combinations for all transformations can be determined unambiguously (situation for curve A in figure 4);

Table 1. Input parameter ranges for all neural networks. The element mass contents are expressed in % and the austenitising temperature (T_{aust}) in °C

Input parameter	minimum	maximum
T_{aust}	850	1350
C	0.10	0.44
Mn	0.50	2.25
Si	0.00	1.00
S	0.000	0.080
P	0.000	0.044
Cr	0.00	1.95
Ni	0.00	2.00
Mo	0.00	0.55
V	0.00	0.45
Cu	0.00	0.48
Al	0.000	0.068
N	0.000	0.050

- if for a particular cooling rate the formation of ferrite does not occur, then ferrite start and end temperatures are given the same value as the pearlite start temperature (situation for curve B in figure 4);
- if for a particular cooling rate both the formation of ferrite and pearlite do not occur, (only bainite and/or martensite are formed) then the start and end temperatures of these transformations are given the same value as the bainite start temperature (situation for curve C in figure 4);
- if only martensite is formed, then all transformation start and end temperatures are given the same value: the martensite start temperature (situation for curve D in figure 4);
- if the formation of bainite does not occur at the particular cooling rate, and only ferrite and pearlite are formed, then the bainite start and end temperature are given the same value as the pearlite end temperature (situation for curve E in figure 4).

It should be stressed that the artificial intercepts assigned to each cooling curve have no physical meaning, but they serve to generate a constant six intercepts for each of the 23 cooling conditions used to convert the CCT diagram from a graphical to a numerical format. The magnitude of the differences between the six predicted intercept temperatures can be used to reconstruct the type of transformation, requiring only a moderate amount of metallurgical knowledge.

Training strategy

In total, 3 neural networks were trained, all on the same data, with different architecture, i.e. with a different number of hidden nodes. A neural network with 5 hidden nodes (network 1), a neural network with 10 hidden nodes (network 2), and a neural network with 15 hidden nodes (network 3) were trained.

As relatively few data (89 steels with measured CCT diagram) were available for training and validation it is unlikely that a randomly chosen validation set is fully representative for the complete data set. In such cases the performance of the neural network is difficult to evaluate and an alternative training procedure must be chosen. It was decided to train the network using cross-validation [10...12]. Each neural network was trained 5 times with different validation sets (each consisting of 18 samples). The overall accuracy in prediction of the neural network is the average obtained after the 5 training sessions. The final neural network can be found by training a neural network with all data in the training set, so without validation set, using the average number of iterations at which overtraining occurred during the 5 cross-validation training sessions.

Training was executed on a IBM compatible PC, 486 DX II, 66 MHz. The maximum number of iterations for all training sessions was pre-set at 1000. However, the best models were already developed after, typically, a 100 iterations.

Overtraining started at these numbers of iteration and the weight factor combination (model) was saved just before the onset of overtraining.

The neural network was trained using the momentum version of the back propagation of error learning rule.

Results and discussion

The accuracy in the prediction of all three neural networks was similar. So for this very complex problem a network with only 5 hidden nodes is sufficient. This neural network (network 1) was chosen to validate the predictive power of the neural network models. The final test for this validation is to compare the measured CCT diagrams with the calculated CCT diagrams. Three of those comparisons will be presented and discussed. One CCT diagram was predicted for a steel in the middle of the input domain (steel 1), a second CCT diagram was predicted for a steel at the low alloy edge of the domain (steel 2), and a third CCT diagram was predicted for a steel at the high-alloy edge of the domain (steel 3). The input parameters for these three predictions are given in **table 2.**

Table 2. Input parameters for three steel grades for the comparison of the predicted and the measured CCT diagram

	T_{aust}	C	Mn	Si	S	P	Cr	Ni	Mo	V	Cu	Al	N
steel 1	890	0.23	0.65	0.30	0.030	0.013	0.12	0.05	0.5	0.03	0.08	0.051	0.000
steel 2	1350	0.10	1.50	0.37	0.007	0.011	0.00	0.00	0.00	0.02	0.00	0.044	0.000
steel 3	1050	0.43	1.67	0.28	0.008	0.021	0.32	0.11	0.03	0.10	0.06	0.000	0.000

The predicted and measured CCT diagrams are shown in **figures 5 to 7.** The shaded areas, surrounded by hand-drawn dotted lines, belong to the experimental CCT diagrams. The squares represent the predicted time-temperature combination for the ferrite formation; the crosses represent the predicted time-temperature combination for the pearlite formation, and the triangles represent the predicted time-temperature combination for the bainite formation. The solid lines through the various data points form the predicted CCT diagram.

The predicted and experimental CCT diagrams of steel 1 are both shown in figure 5. The martensite start temperature was well predicted. The prediction of the bainite start temperature was also predicted with high accuracy. Only at those cooling rates at which bainite was the first phase to form from austenite (the bainite nose), the predictions were less accurate. The prediction of the ferrite start temperature was 25 °C too low, and it was also predicted at lower cooling rates. The same holds for the prediction of the pearlite start temperature. The bainite end temperature was predicted with high accuracy, except for the low cooling rates. The reason for this can be found in the data processing as will be shown later in the discussion.

The predicted and experimental CCT diagrams for the low carbon steel (steel 2) are both shown in figure 6. Again, the martensite start temperature was predicted with high accuracy. The onset of the transformation of austenite to ferrite or bainite was predicted at too high a temperature. The difference between predicted and measured temperatures was between 25 and 50 °C. The pearlite start temperatures are accurate, however, a much smaller transformation area was predicted (a higher temperature for the pearlite end transformation was predicted). The prediction of the end temperature of the bainite formation was also too high (50 °C) and the formation of bainite was predicted at the lower cooling rates, at which no bainite formation was measured. Again, the reason for this disagreement can be found in the data processing. Summarising, the prediction of the CCT diagram for the low-carbon, low-alloyed steel (steel 2) was less accurate than that of the steel in the middle of the input domain (steel 1), but still quite acceptable.

The predicted and experimental CCT diagrams for the steel with the higher alloy content (steel 3) are both shown in figure 7. For this steel grade the predicted martensite start temperature was ~ 40 °C too high. The first transformation of austenite to ferrite or bainite was predicted at higher temperatures (maximum difference is 25 °C) and the formation of bainite was predicted at higher cooling rates than has been measured. The prediction of the pearlite start temperature was good. The pearlite end temperature was predicted at too high a level (difference up to 100 °C), as was the case for steel 2. The same holds for the bainite start temperature at the lower cooling rates. The predicted bainite end temperatures were fairly accurate. Again, the prediction of the CCT diagram of steel 3 was less accurate than that of steel 1, but still very acceptable. Especially when taking into account the limited number of data sets available for training and the intrinsic variance in the experimental CCT diagrams.

A more quantitative way to evaluate the performance of the neural networks is by looking at the relative standard deviation, s, of all 138 (23 sets of 6 intercepts) predictions on which the predicted CCT diagrams are constructed for the steel grades in the validation set. s is defined as:

$$s = \sqrt{\sum_{i=1}^{89} \frac{\left(y_{t,i} - y_{p,i}\right)^2}{(89-1)}} \qquad (1)$$

with $y_{t,i}$ - measured transformation temperature and $y_{p,i}$ - predicted transformation temperature for sample i, resp.

All three neural network models gave similar values for s. The s values for the transformation temperature predictions for network 1 are given in **table 3.**

The error in the prediction of the transformation start temperature for the fast and the slow cooling rates is lower than for the intermediate ones. The reason for this is two-fold:

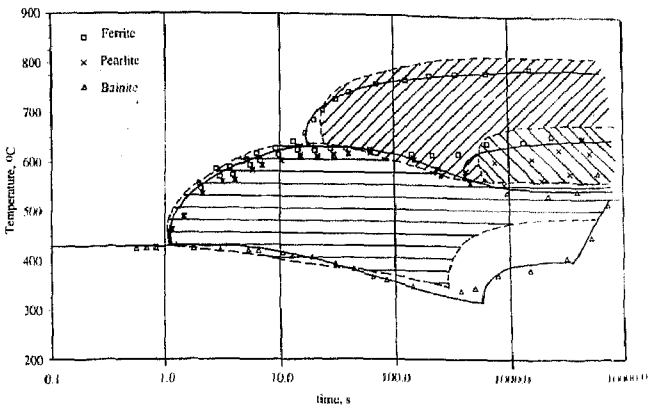

Figure 5. Predicted and experimental CCT diagram of steel 1

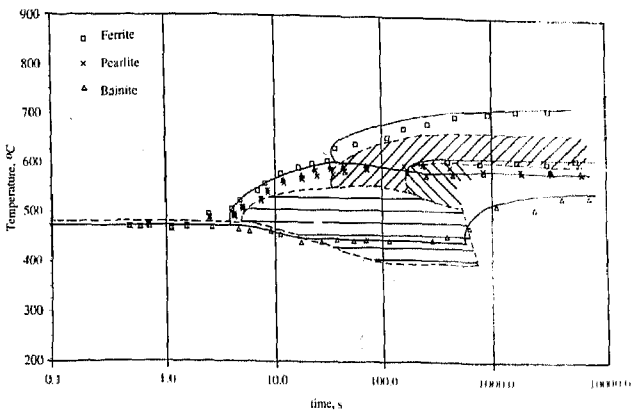

Figure 6. Predicted and experimental CCT diagram of steel 2

Table 3. Error of the various predicted transformation temperature predictions (°C) of network 1. The cooling rates are expressed in °C/s

Cooling rate	ferrite		pearlite		bainite	
	start	end	start	end	start	end
713	46	46	45	46	45	46
583	45	46	46	46	46	46
457	46	45	45	46	46	45
309	56	48	48	48	48	45
220	68	58	59	58	60	45
133	83	70	70	70	71	44
67	90	76	74	72	72	48
62	94	75	75	72	73	48
36	93	73	76	72	73	53
32	91	72	75	70	71	46
22	86	65	67	64	64	45
14	80	61	64	60	62	52
10	78	58	59	58	60	58
7.0	77	58	63	60	63	66
5.5	62	48	53	46	53	75
3.3	63	47	48	42	53	92
1.2	58	44	43	42	45	106
0.96	52	42	45	48	52	112
0.59	49	42	49	52	58	130
0.30	42	44	53	58	72	138
0.13	42	46	57	56	82	127
0.072	42	44	56	57	79	114
0.047	44	42	56	55	82	117

- one, the transformation process for the intermediate cooling rates itself is more complex than for the faster and slower ones. When quenched, the austenite will always transform to martensite. When slowly cooled, the austenite will always first (partially) transform to ferrite. The chemical composition of the steel is of little importance compared to the cooling conditions at these cooling rates. For the intermediate cooling rates, the phase to be formed from austenite will depend more strongly on the chemical composition. The austenite may transform to martensite, bainite, ferrite, or even directly to pearlite in the case of a eutectoid steel, with only small variations in composition;
- two, the cooling curves intersect the transformation curves in the CCT diagram at an angle close to 90 ° for the high and low cooling rates. This angle is much smaller for the intermediate cooling rates. Now a small shift in the transformation curve on the time axis will result in a relatively large error in the intercept temperature. This is clearly an artefact due to the procedure used to convert the CCT diagram into numerical data.

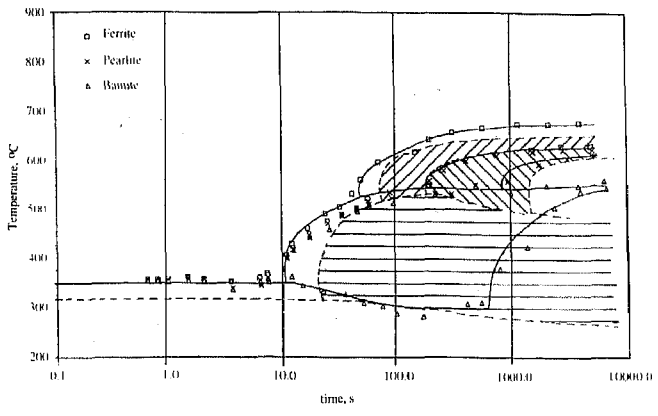

Figure 7. Predicted and experimental CCT diagram of steel 3

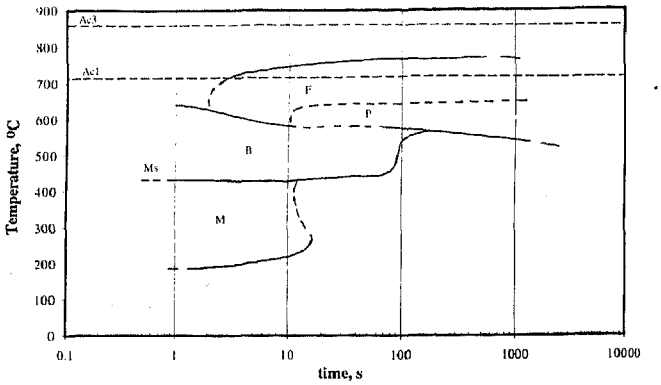

Figure 8. CCT diagram of a 0.14% C, 1.53% Mn, 0.36% Si, 0.008% S, 0.009% P, 0.06% Cr, 0.03% Ni, 0.01% Mo, 0.04% V, 0.02% Cu, 0.057% Al steel [4]

The error in the prediction of the bainite start and end temperatures for the lower cooling rates rises to a level of over 100 °C. The explanation for this high *s*-value is that bainite will not form at these cooling rates. However, due to our sampling procedure, bainite is always assumed to be present, be it at the pearlite end temperature only. Such data handling clearly introduced an inconsistency in the data set.

However, a more important reason for the still relatively high error in the predictions is due to inconsistency in the original data from literature as will be shown below.

The experimental CCT diagrams in **figures 3 and 8** are of steels with almost identical chemical compositions. However, the CCT diagrams, which were determined by different institutes are markedly different. Clearly, results obtained by different institutes for nominally the same steel grade might differ due to minor differences in measurement procedures. Similarly, the diagrams in **figures 9 and 10** are of the very same steel, however, with different austenitising temperatures. The austenitising temperature was included as an input parameter, but the differences in these CCT diagrams are bigger than can be accounted for by the different austenitising temperatures. These 4 diagrams were merely included to illustrate that the data used for training and validation of the network were to some extent inconsistent, intrinsically limiting the predictive power of the neural network. Five possible reasons for the inconsistency in the data are given:

- the interpretation of the dilatometer curves and the final construction of the CCT diagram based on these dilatometer measurements may vary from person to person. A lot of personal bias can be put in both analyses;
- an unknown temperature difference might exist over the dilatometer sample, resulting in an incorrect tem-

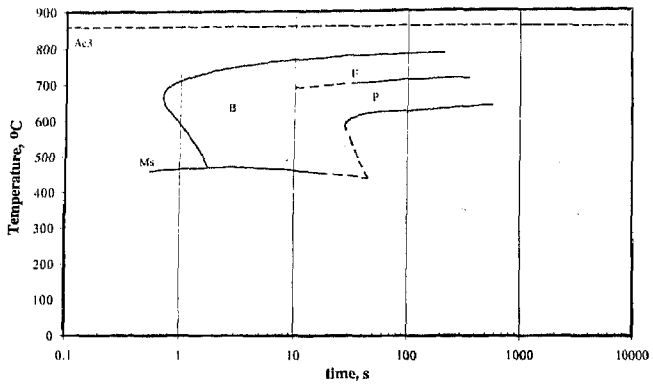

Figure 9. CCT diagram of a 0.11% C, 1.23% Mn, 0.31% Si, 0.018% S, 0.031% P, 0.08% V, 0.005% N steel [4]

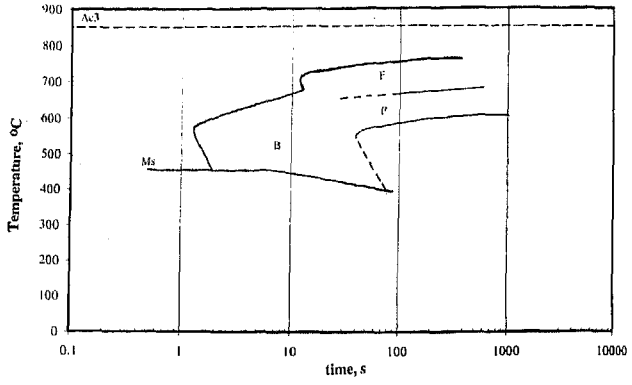

Figure 10. CCT diagram of a 0.11% C, 1.23% Mn, 0.31% Si, 0.018% S, 0.031% P, 0.08% V, 0.005% N steel [4]

perature measurement (it is common to have only one thermocouple attached to the sample);
- the size of the dilatometer samples is very small and they may not be representative for the bulk of the material;
- decarburisation of the sample is known to occur often unnoticed;
- the prior austenite grain size could not be included in the model, for lack of suitable input data. It is known that at the same austenitization temperature different austenite grain sizes can be obtained. Hence the use of the austenitization temperature as in our model is not sufficient.

The above all contribute to the inconsistency of the data used for training and validation of the network.

Having verified that the predictions of the neural network are as accurate as the scatter in the input data allows, the influence of the various input parameters on the CCT diagram can be investigated. The predicted effects of the various element concentrations on the shape of the CCT diagram can not be shown in simple plots because of the many lines in a CCT diagram and the multi-variate nature of the input. Just as an illustration, both the influence of carbon and manganese on the start of the austenite decomposition, the meta-stable Ar_3 temperature, are shown in **figures 11 and 12.** The base composition of these steels (i.e. the concentrations of all alloying element except carbon and manganese) was equal to that of steel 1.

The influence of the carbon content on the Ar_3 temperature is shown in figure 11. The solid lines are hand-drawn for three different carbon contents (0.05, 0.25, and 0.45%) to bring out the different types of transformation more clearly. This figure illustrates the well known lowering of the Ar_3 temperature with increasing carbon concentration. The influence of carbon on the martensite start temperature in this subset equals that of earlier work [2] using a different type of analysis: a decrease of 225 °C per percent carbon for carbon concentrations less than 0.40%.

The influence of the manganese content on the Ar_3 temperature is shown in figure 12 for three different manganese concentrations (0.75, 1.50, and 2.25%). Manganese lowers the Ar_3 temperature too, but the effect is less strong than that of carbon. The martensite start temperature is lowered by 30 °C per percent manganese, in agreement with earlier work [2]. The influence of manganese is stronger at intermediate and lower cooling rates when diffusional redistribution takes place [13; 14].

The influence of both carbon and manganese was discussed, merely to illustrate the potential of the neural network model. It is now possible to predict a transformation line in the CCT diagram for steel grades inside the domain given in table 1 within just a few seconds. The effects of varying single element concentration without contributions from others can be investigated, something almost impossible in practice.

While in the present work a comparison between the predicted transformation start and finish lines and the experimental curves in the original data set has been made

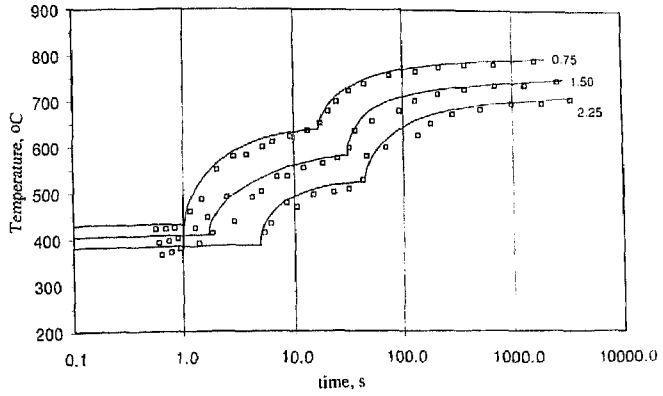

Figure 11. Influence of the carbon content on the Ar_3

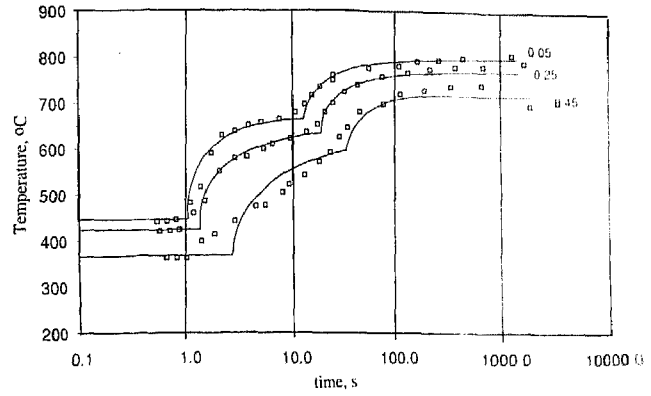

Figure 12. Influence of the manganese content on the Ar_3

only, a more extensive comparison of the performance of this neural network model with the existing metallophysical models for CCT transformation line predictions would be desirable. It should be realized that such a comparison will be hampered by the fact that each of the models has been validated for different steel grades and models will have to be used outside their validated domains. This wider comparison of transformation models is outside the scope of this article and will have to be made in a future article.

Conclusion

It is possible to predict the transformation start and finish lines in CCT diagrams on basis of the chemical composition (12 alloying elements) and the austenitising temperature using artificial neural networks. The number of hidden nodes did not influence the accuracy in the predictions. A network with just five hidden nodes was used to evaluate the performance of the neural network models. The error in the temperature prediction depends on the cooling rate. For high and low cooling rates, the error is only ~ 40 °C. For the intermediate cooling rates the error in the temperature prediction is higher, mainly due to the shape of the CCT diagrams themselves.

The predictive power of the neural networks is more than satisfactory and all general trends are well predicted. The prediction of the fine detail is seriously hindered by the inconsistency within the data set used for the training and validation. With the neural networks trained, it is possible to investigate pure relations between input parameters and CCT diagram easily, something not generally possible in practice.

Acknowledgements

W.G. Vermeulen wishes to thank Dr. A.A. Howe of British Steel plc, for the possibility to work for a period of three months at British Steel plc., Swinden Technology Centre, Moorgate, Rotherham. Thanks is also expressed to Ir. P.J. van der Wolk for his assistance in the preparation of the figures.

(A 01 178; received: 11. April 1996;
in revised form: 25. July 1996)

References

[1] *Sachs, K*: Heat Treatment of Metals 2 (1975) No. 174, p. 43/57.
[2] *Vermeulen, W.G.; Morris, P.F.; Weijer, A.P. de; Zwaag, S. van der*: Ironmak. Steelmak. 23 (1996), to be published.
[3] *Vermeulen, W.G.; Wolk, P.J. van der; Weijer, A.P. de; Zwaag, S. van der*: Journ. Mater. Eng. Performance 5 (1996) No .1, p. 57/63.
[4] Atlas of Continuous Cooling Diagrams for Vanadium Steels, Vanitec, Kent, 1985.
[5] *Rumelhart, D.E.; McCleland J.L.; et al.*: Parallel distributed processing, 8th edn., MIT Press, Cambridge (MA), 1986, Vol. 1.
[6] *Hecht-Nielsen, R.*: Neurocomputing, Addison-Wesley Publishing Company, Inc. Reading, Massachusetts, 1991.
[7] *Aleksander, I.; Morton, H.*: An introduction to Neural Computing, Chapmann & Hall, London, 1993.
[8] *Zupan, J.; Gasteiger, J.*: Neural Networks for Chemists, An Introduction, VCH Publishers, New York, USA, 1993.
[9] *Atkins, M.*: Atlas of Continuous Cooling Transformation Diagrams for Engineering Steels, British Steel Corporation, Rotherham, 1977.
[10] *Allen, D.*: Technometrics 16 (1974), p. 125/27.
[11] *Geisser, S.*: Journ. Americ. Statistic. Assoc. 10 (1975), p. 320/28.
[12] *Stone, M.*: Journ. Royal Statistic. Soc. 36 (1974), p. 111/33.
[13] *Kirchner, G.; Nishizawa, T.; Uhrenius, B.*: Met. Trans. 4 (1973), p. 167/74.
[14] *Huang, W.*: CALPHAD 13 (1989), p. 243/52.